Colloids and Surfaces B: Biointerfaces 102 (2013) 472–478

Contents lists available at SciVerse ScienceDirect

Colloids and Surfaces B: Biointerfaces

journal homepage: www.elsevier.com/locate/colsurfb

Examination of fluorination effect on physical properties of saturated long-chain alcohols by DSC and Langmuir monolayer

Hiromichi Nakahara[a], Shohei Nakamura[b], Yoshinori Okahashi[a], Daisuke Kitaguchi[a], Noritake Kawabata[a], Seiichi Sakamoto[a], Osamu Shibata[a,*]

[a] Department of Biophysical Chemistry, Faculty of Pharmaceutical Sciences, Nagasaki International University, 2825-7 Huis Ten Bosch, Sasebo, Nagasaki 859-3298, Japan
[b] Department of Pharmaceutical Technology, College of Pharmaceutical Sciences, Matsuyama University, 4-2 Bunkyo-cho, Matsuyama, Ehime 790-8578, Japan

ARTICLE INFO

Article history:
Received 1 August 2012
Received in revised form 17 August 2012
Accepted 17 August 2012
Available online xxx

Keywords:
Fluorinated amphiphile
Fatty alcohol
Langmuir monolayer
DSC
Surface pressure
Surface potential

ABSTRACT

Partially fluorinated long-chain alcohols have been newly synthesized from a radical reaction, which is followed by a reductive reaction. The fluorinated alcohols have been investigated by differential scanning calorimetry (DSC) and compression isotherms in a Langmuir monolayer state. Their melting points increase with an increase in chain length due to elongation of methylene groups. However, the melting points for the alcohols containing shorter fluorinated moieties are lower than those for the typical hydrogenated fatty alcohols. Using the Langmuir monolayer technique, surface pressure (π)-molecular area (A) and surface potential (ΔV)–A isotherms of monolayers of the fluorinated alcohols have been measured in the temperature range from 281.2 to 303.2 K. In addition, a compressibility modulus (Cs^{-1}) is calculated from the π–A isotherms. Four kinds of the alcohol monolayers show a phase transition (π^{eq}) from a disordered to an ordered state upon lateral compression. The π^{eq} values increase linearly with increasing temperatures. A slope of π^{eq} against temperature for the alcohols with shorter fluorocarbons is unexpectedly larger than that for the corresponding fatty alcohols. Generally, fluorinated amphiphiles have a greater thermal stability (or resistance), which is a characteristic of highly fluorinated or perfluorinated compounds. Herein, however, the alcohols containing perfluorobutylated and perfluorohexylated chains show the irregular thermal behavior in both the solid and monolayer states.

1. Introduction

Perfluorinated compounds are considerably different from their original compounds in bulkiness, helical conformation, and stiffness [1]. Fluorocarbon chains (*F*-chains) are more hydrophobic than hydrocarbon chains (*H*-chains) [2]. Moreover, the lower polarizability of fluorine (ca. 0.557) in *F*-chains generates very weak inter-chain van der Waals interactions [3], and fluorinated compounds are also chemically and thermally more stable. These properties consequently bring about lower surface tensions and higher vapor pressures. However, perfluorinated compounds have a tendency to accumulate in the human body and the environment [4–7]. Nevertheless, perfluorooctylbromide (PFOB) has been investigated for oxygen delivery system and shows short organ retention [8,9]. Thus, the amphiphiles with short *F*-chains ($n_F \leq 8$) are considered to be acceptable in the clinical field. In the previous study, we have reported that partially fluorinated alcohols of $CF_3(CF_2)_7(CH_2)_mOH$ ($m = 5$ and 11) are incorporated into pulmonary surfactant model preparations to improve their effectiveness [10]. In addition, highly fluorinated amphiphiles have multiple applications in materials science as well as a biomedical field [11–13]. In this regard, the compounds containing both fluorinated and hydrogenated moieties have certain potential application in many fields. However, their fundamental properties such as solubility in various solvents, crystalline structure, and phase behavior are still poorly documented. In particular, it has not been made clear yet how the degree of fluorination in a molecule affects its original properties. There are a few reports on partially fluorinated fatty acids [14–16]. However, dissociation of their carboxyl groups makes the effect of fluorination degree ambiguous and unclear due to the great difference in p*K*a between them and the corresponding hydrogenated fatty acids. Thus, the authors have paid attention to partially fluorinated alcohols [$CF_3(CF_2)_{n-1}(CH_2)_mOH$, abbrev. *FnHm*OH], which have a hydroxyl group of very weak acid under a normal aqueous environment. To our knowledge, surface properties of *F*6*H*10OH, *F*8*H*5OH, and *F*8*H*11OH have been reported [17,18], and, however, there are no systematic investigations to overcome the issue mentioned above.

* Corresponding author at: Department of Biophysical Chemistry, Faculty of Pharmaceutical Sciences, Nagasaki International University, 2825-7 Huis Ten Bosch, Sasebo, Nagasaki 859-3298, Japan. Tel.: +81 956 20 5686; fax: +81 956 20 5686.
E-mail addresses: wosamu@niu.ac.jp, wosamu-s@hotmail.co.jp (O. Shibata).
URL: http://www.niu.ac.jp/~pharm1/lab/physchem/indexenglish.html (O. Shibata).

0927-7765/$ – see front matter © 2012 Elsevier B.V. All rights reserved.
http://dx.doi.org/10.1016/j.colsurfb.2012.08.031

The present paper intends to report characterization of *FnHm*OH in the solid state as well as the monolayer state. First, we chemically synthesize a series of *FnHm*OH using the method described by Takai et al. [19]. Commonly, in the present synthesis the radical reaction is widely employed, where azobisisobutyronitrile (AIBN) is used as a radical initiator, and the temperature of oil bath needs to be kept at 80–260 °C depending on a product species. In the current method, however, the radical reaction can occur in the absence of AIBN even at room temperatures. Second, effects of the fluorination degree in *FnHm*OH on its physical properties have been investigated by differential scanning calorimetry (DSC) in a solid state and by compression isotherms in a Langmuir monolayer state. Melting point and enthalpy change of fusion for *FnHm*OH are assessed from the DSC traces. In the monolayer study, surface pressure (π)–molecular area (A) and surface potential (ΔV)–A isotherms of *FnHm*OH are measured on water in the temperature range from 281.2 to 303.2 K. Thermodynamic parameters such as enthalpy and entropy changes on phase transition from a disordered to an ordered state are calculated from the π–A isotherms. Furthermore, an elasticity of the monolayers is elucidated by a compressibility modulus (Cs^{-1}).

2. Materials and methods

2.1. Materials

(Perfluorooctyl) pentanol (*F8H5*OH) and (perfluorooctyl) undecanol (*F8H11*OH) were synthesized as reported previously [20]. (Perfluorobutyl) undecanol (*F4H11*OH), (perfluorohexyl) heptanol (*F6H7*OH), (perfluorohexyl) nonanol (*F6H9*OH), (perfluorohexyl) undecanol (*F6H11*OH), (perfluorooctyl) heptanol (*F8H7*OH), and (perfluorooctyl) nonanol (*F8H9*OH) were newly synthesized (see Supplementary Materials). These partially fluorinated alcohols (*FnHm*OH) were purified by repeated recrystallizations from acetone/H_2O mixed solvents and their identification was checked by ^{1}H NMR, ^{13}C NMR (JNM-AL400, Jeol, Tokyo, Japan), elemental analysis, and FAB-MS (SX102A, Jeol); m/z 391.1685 $[M+H]^+$ for *F4H11*OH. Their purity (>99%) was determined by GC–MS (QP-1000, Shimadzu, Kyoto, Japan), which is based on relative peak area. Perfluorobutyl iodide (purity > 95%) and perfluorohexyl iodide (>95%) were purchased from Daikin Industries, Ltd. (Osaka, Japan). Perfluorooctyl iodide (97%) was obtained from Fluorochem Ltd. (Derbyshire, United Kingdom). 6-Hepten-1-ol (>96%), 8-nonen-1-ol (>97%), and 10-undecen-1-ol (>98%) were purchased from Tokyo Chemical Industry Co. Ltd. (Tokyo, Japan). These reagents were used without further purification. Chloroform (99.7%) and methanol (99.8%) used as spreading solvents for a monolayer study were obtained from Cica-Merck (Uvasol, Tokyo, Japan) and nacalai tesque (Kyoto, Japan), respectively. The water used for synthesis and isotherm measurement was thrice distilled (the surface tension = 71.99 mN m^{-1} at 298.2 K and the electrical resistivity = 18 MΩ cm).

2.2. Differential scanning calorimetry

Differential scanning calorimetry (DSC) experiments were made by a DSC8230 (Rigaku, Tokyo, Japan). Ten milligrams of the solid samples was placed in an aluminum pan, and then the pan was sealed with a hermetic sealer. Prior to measurement, the solid sample was once molten to reduce the influence of polymorphism. Purified indium and water were used as the standard calibration sample for enthalpy change. Samples were heated at the rate of 1 K min^{-1}. The melting points were determined as the temperature at the intersection point between the endothermic peak line for phase transition and the baseline as reported previously [16,21].

2.3. Surface pressure–molecular area isotherms

The surface pressure (π) of monolayers was measured using a commercially available film balance system (KSV Minitrough, KSV Instruments Ltd., Finland). The surface pressure sensor had a resolution of 0.004 mN m^{-1}. The pressure-measuring system was equipped with filter paper (Whatman 541, periphery = 2.0 cm). The trough was made from Teflon (area = 273 cm^2), and Teflon barriers were used in this study. The π–molecular area (A) isotherms on the subphase of water were recorded at 281.2–303.2 K with precision of 0.1 K. Stock solutions of *FnHm*OH (1.0 mM) were prepared in chloroform/methanol (2/1, v/v). The spreading solvents were allowed to evaporate for 15 min prior to compression. The monolayer was compressed at a barrier speed of 10 mm min^{-1}, or a compressing speed of ~0.08 nm^2 molecule^{-1} min^{-1}. The standard deviations (SD) for molecular surface area and surface pressure were ~0.01 nm^2 and ~0.1 mN m^{-1}, respectively.

2.4. Surface potential–molecular area isotherms

The surface potential (ΔV) was recorded simultaneously with surface pressure, when the monolayer was compressed at the air/water interface. It was monitored with a Kelvin probe system (KSV SPOT1, KSV Instruments Ltd.) at 1–2 mm above the interface, while a counter electrode was dipped in the subphase. The resolution and SD for the surface potential were 1 and 5 mV, respectively.

3. Results and discussion

3.1. Synthesis of FnHmOH

Partially fluorinated long-chain alcohols (*FnHm*OH) were synthesized by the following procedures (see Scheme 1 and Supplementary Materials) [19]. ω-Unsaturated alkanols reacted with perfluoroalkyl iodides in the presence of $Na_2S_2O_4$, which is a free radical initiator [22,23], to give fluorinated iodoalkan-1-ols in 58–86% yield. These compounds were deiodinated with Zn in the presence of $NiCl_2{\cdot}6H_2O$ to give crudes of *FnHm*OH. They were purified with a column chromatography and a recrystallization to give *FnHm*OH in 78–97% yield. Through both the two steps, chemical reactions can take place at room temperatures as opposed to use of AIBN as a radical initiator. In addition, similarly to the synthesis method using AIBN, the present method relatively gives a high yield of fluorinated iodoalkan-1-ols.

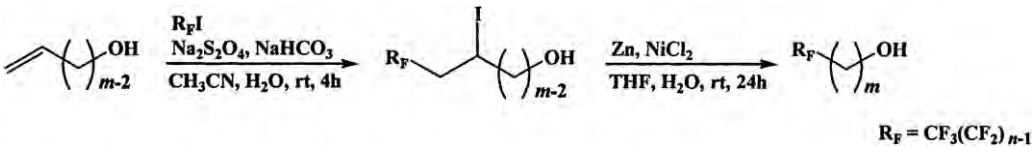

Scheme 1. Synthesis of *FnHm*OH from ω-unsaturated alkanols with perfluoroalkyl iodides.

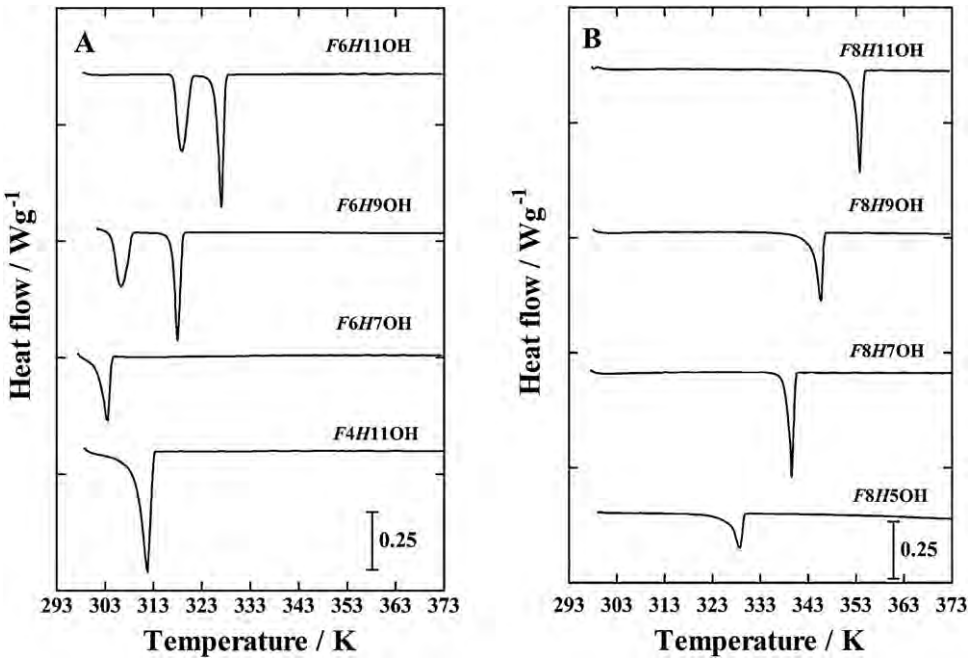

Fig. 1. DSC traces of solids of (A) *F4H*11OH, *F6Hm*OH (m = 7, 9, 11) and (B) *F8Hm*OH (m = 5, 7, 9, 11).

3.2. Characterization of FnHmOH

3.2.1. Thermal analysis

DSC curves for *FnHm*OH solids are shown in Fig. 1. All the *FnHm*OH solids have well-defined endothermic peaks at different temperatures. The transitions represent absorption of heat. A pre-transition (or phase transition of solid), which is in common followed by the main transition (melting), is observed for *F6H*9OH and *F6H*11OH (Fig. 1A) while *F8Hm*OH has only one peak (Fig. 1B). In addition, the peaks at the melting are considerably sharp due to the high purity of the samples.

Fig. 2 shows the change of melting point of *FnHm*OH obtained from DSC curves against total carbon number including fluorocarbons. The melting points of *F6Hm*OH and *F8Hm*OH increase almost linearly with an increase in total carbon number. As for the degree of fluorination in *FnHm*OH molecules, the highly fluorinated alcohols indicate higher melting points; *F4H*11OH < *F6Hm*OH < *F8Hm*OH. This supports a fact that fluorocarbon is more stabilized energetically than hydrocarbon. In the case of typical 1-alkanols ($(CH_3)(CH_2)_{m-1}OH$, *Hm*OH), their melting points monotonously increase with increasing total carbon atoms [24]. However, the melting points of *F4H*11OH and *F6Hm*OH are lower than those of *Hm*OH. This phenomenon is an unexpected behavior in terms of the energetic stabilization of fluorinated compounds. According to the weak van der Waals interaction between fluorocarbons, *F8Hm*OH should exhibit lower melting temperatures than *Hm*OH. However, the melting points of perfluorinated fatty acids are higher than those of the corresponding fatty acids [25]. More detail analysis of this irregular behavior is under investigation with a X-ray diffraction (XRD) and a small angle X-ray scattering (SAXS), which will be reported in the subsequent paper. Nevertheless, it is made clear that the homologous interaction for *F4H*11OH and *F6Hm*OH in the solid state is expected to be considerably different from that for *F8Hm*OH and the ones containing a longer *F*-chains.

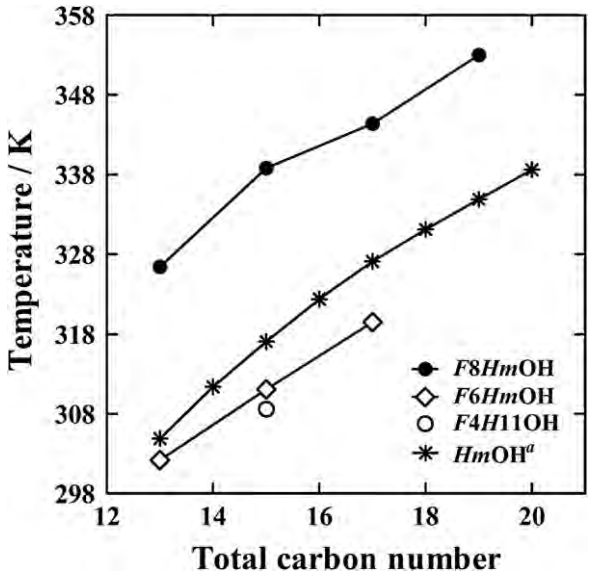

Fig. 2. Changes in melting point of *FnHm*OH (n = 4, 6, 8, m = 5, 7, 9, 11) and *Hm*OH (m = 13–20) against total carbon number. [a]From Ref. [24].

The total enthalpy change (ΔH) of phase transition and fusion (melting) against total carbon number is shown in Fig. 3. The ΔH values of *F6Hm*OH and *F8Hm*OH monotonously increase with increasing the number of carbon atoms. As for *Hm*OH, their ΔH values also increase linearly with an increase in total carbon number [26]. Unexpectedly, *F6Hm*OH exhibits almost the same ΔH values as *F8Hm*OH at the same number of carbon atoms irrespective of the different degree of fluorination. This result suggests that there is few difference in stability between *F6Hm*OH and *F8Hm*OH in solid state. However, *F4H*11OH has a larger ΔH value than the other two fluorinated samples, which means the higher crystalline stability of *F4H*11OH. Furthermore, the contribution per methylene group of an (fluorinated) n-alkyl chain to the enthalpy change (ΔH_{CH_2}) is evaluated to be 2.1 kJ mol^{-1} for *F6Hm*OH and *F8Hm*OH, and 4.8 kJ mol^{-1} for *Hm*OH from the slope in the figure. These values mean that the fluorinated moiety in a molecule depresses the stability of crystals made of the homologous molecules.

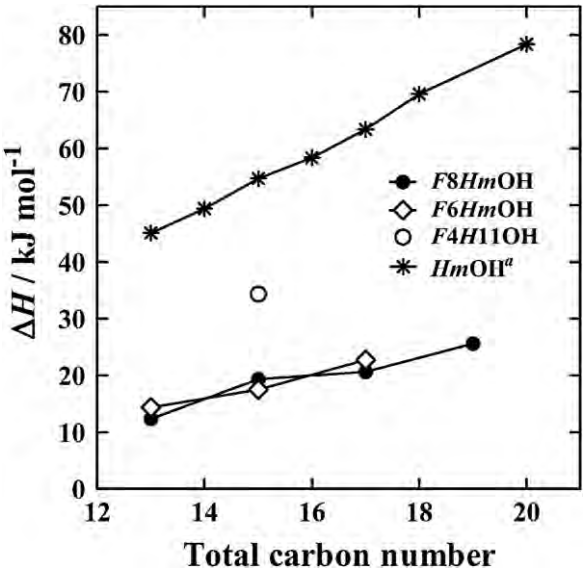

Fig. 3. The total enthalpy changes of fusion and phase transition (ΔH) for *Fn*H*m*OH ($n = 4, 6, 8, m = 5, 7, 9, 11$) and *Hm*OH ($m = 13$–$20$) against total carbon number. [a]From Ref. [26].

3.3. Langmuir monolayer study

The representative surface pressure (π)–molecular area (A) and surface potential (ΔV)–A isotherms of *Fn*H*m*OH at different temperatures on water are collected (Fig. 4). *F*4*H*11OH forms unstable monolayers at 303.2 K on water due to the high solubility to the subphase (data not shown). The *F*4*H*11OH monolayer at 283.2 K shows a phase transition (π^{eq}) from disordered to ordered states at ~4 mN m^{-1}, which is indicated by an arrow (Fig. 4A). In general, the kink point of the transition on π–A isotherms for fluorinated compounds is unclear compared with that for typical hydrogenated amphiphiles [27,28]. Accordingly, the phase behavior of fluorinated monolayers in the disordered/ordered coexistence state is difficult to be visually caught with the *in situ* microscopic techniques such as Brewster angle microscopy (BAM) and fluorescence Microscopy (FM) [29]. In the present study, the BAM observations for *F*4*H*11OH, *F*6*H*7OH, *F*6*H*9OH, and *F*8*H*5OH monolayers reveal optically homogeneous images in the coexistence state (data not shown). This is because of the formation of considerably small ordered domains induced by weak van der Walls interaction [28]. After the transition, the monolayer undergoes a collapse at ~49 mN m^{-1} upon further compression, where the monolayer transforms from two-dimensional to three dimensional states such as bilayer and multilayer. On the other hand, the ΔV value, which is related with dipole moment perpendicular to the surface in the Helmholtz equation and thus reflects the monolayer orientation, decreases negatively upon lateral compression and finally approaches to ~−700 mV at the close-packed state. The ΔV–A isotherms express a change in molecular orientation upon compression. The ΔV value in common indicates positive variation for hydrogenated lipid monolayers. However, the isotherms of fluorinated compounds show the opposite sign or negative variation due to the electronegativity based on a fluorine as the molecular areas decrease [27,29,30]. A compressibility modulus (or dilatational elasticity modulus, Cs^{-1}) is calculated from the π–A isotherm by the following equation:

$$Cs^{-1} = -A\left(\frac{\partial \pi}{\partial A}\right)_T \quad (1)$$

The Cs^{-1}–π curves for *F*4*H*11OH show more distinct kinks corresponding to the transition compared with the π–A isotherms, which are indicated by arrows (see the inset). In addition, The Cs^{-1} values give information on the monolayer packing on compression. A high compressibility modulus (or low compressibility) is a sign of the tight packing and the large cohesive forces between components of monolayers. According to the Davies and Rideal classification [31], the values in $12.5 < Cs^{-1}$ (in mN m^{-1}) < 50 and $100 < Cs^{-1} < 250$ evidence that the monolayer is in a liquid-expanded (LE) state and a liquid-condensed (LC) state, respectively. Although the classification is defined for typical lipid monolayers, it is also valid for the monolayers of fluorinated amphiphiles. As seen in the Cs^{-1}–π curves (the inset of Fig. 4A), the π^{eq} values increase as temperature rises. More detail analysis on the transition is performed in the latter section. The rise of temperature induces a slight reduction of the collapse pressures by ~2 mN m^{-1} due to the improvement of a molecular motion and exerts few influences on the ΔV values. The limiting (or extrapolated) area, which can be obtained from π–A isotherms by extrapolation of the straight-line in the condensed state to the area axis at $\pi = 0$, increases from 0.32 nm^2 (283.2 K) to 0.40 nm^2 (298.2 K). These values coincide nearly with the cross-section of a perfluorocarbon chain (~0.28 nm^2) [2]. Thus, the molecular area of *F*4*H*11OH monolayers contributes strongly to the perfluorobutyl chain.

*F*6*H*m*OH has a tendency to form tightly packed monolayers with an increase in m (Fig. 4B–D). Note that the monolayers of $m = 7$ at 293.2 K and $m = 9$ at 303.3 K (data not shown) are less stable for the reproducibility and the extrapolated area. The transition from the disordered to ordered phases is observed for $m = 7$ and 9, not for $m = 11$. With increasing temperatures, the π^{eq} values increase and the collapse pressures slightly decrease by ~2 mN m^{-1} similarly to *F*4*H*11OH. The ΔV values at the close-packed state are in the range from −650 to −720 mV for the whole *F*6*H*m*OH monolayers. The extrapolated areas are included in the small range of 0.33–0.36 nm^2 regardless of temperature. These results reveal that the *F*6*H*m*OH monolayer takes on the stronger thermal resistance than the *F*4*H*11OH monolayer.

In the case of *F*8*H*m*OH (Fig. 4E–G), the monolayer of $m = 5$ exhibits the phase transition. The data for $m = 5$ at 293.2 K agree well with those reported in the previous papers [17,29]. The monolayer of $m = 5$ above 298.2 K is unstable. Although the isotherms of $m = 7$ at 303.2 K are precisely reproduced, the monolayer is less stable on water due to the relative small limiting area (~0.29 nm^2). Typical ordered monolayers are formed for $m = 7$ and 9. As for the longer fluorinated alcohol of *F*8*H*11OH, it has been reported to be in ordered phases from low to high surface pressures upon compression [32]. Among the *Fn*H*m*OH molecules studied, *F*8*H*m*OH monolayers indicate the highest collapse pressure, the largest Cs^{-1} value, and the most negative ΔV value (−700 to −800 mV) at the close-packed state, which means that they can form the most tightly packed and stable monolayers against temperature. It has been widely accepted as the three-layer model proposed by R.J. Demchak and T. Fort that the ΔV value at the close-packed monolayer is nearly independent of hydrophobic chain length in a molecule [33]. As for the monolayers of perfluorocarboxylic acids, the minimum ΔV value converges to ~−1000 mV irrespective of the elongation of fluorocarbon chains [27]. Herein, the slight decrease in minimum ΔV value reflects the stronger cohesion of perfluorooctyl moieties, and consequently *F*8*H*m*OH is possible to form the more tightly packed monolayer. Nevertheless, there are few temperature dependences of the collapse pressure, the extrapolated area (0.31–0.35 nm^2), and the minimum ΔV value similarly to the other *Fn*H*m*OH, which supports the thermal resistance in the monolayer state.

Fig. 5 shows the plots of π^{eq} values against temperature for *F*4*H*11OH, *F*6*H*7OH, *F*6*H*9OH, and *F*8*H*5OH monolayers. The π^{eq} values for all the compounds here increase linearly with

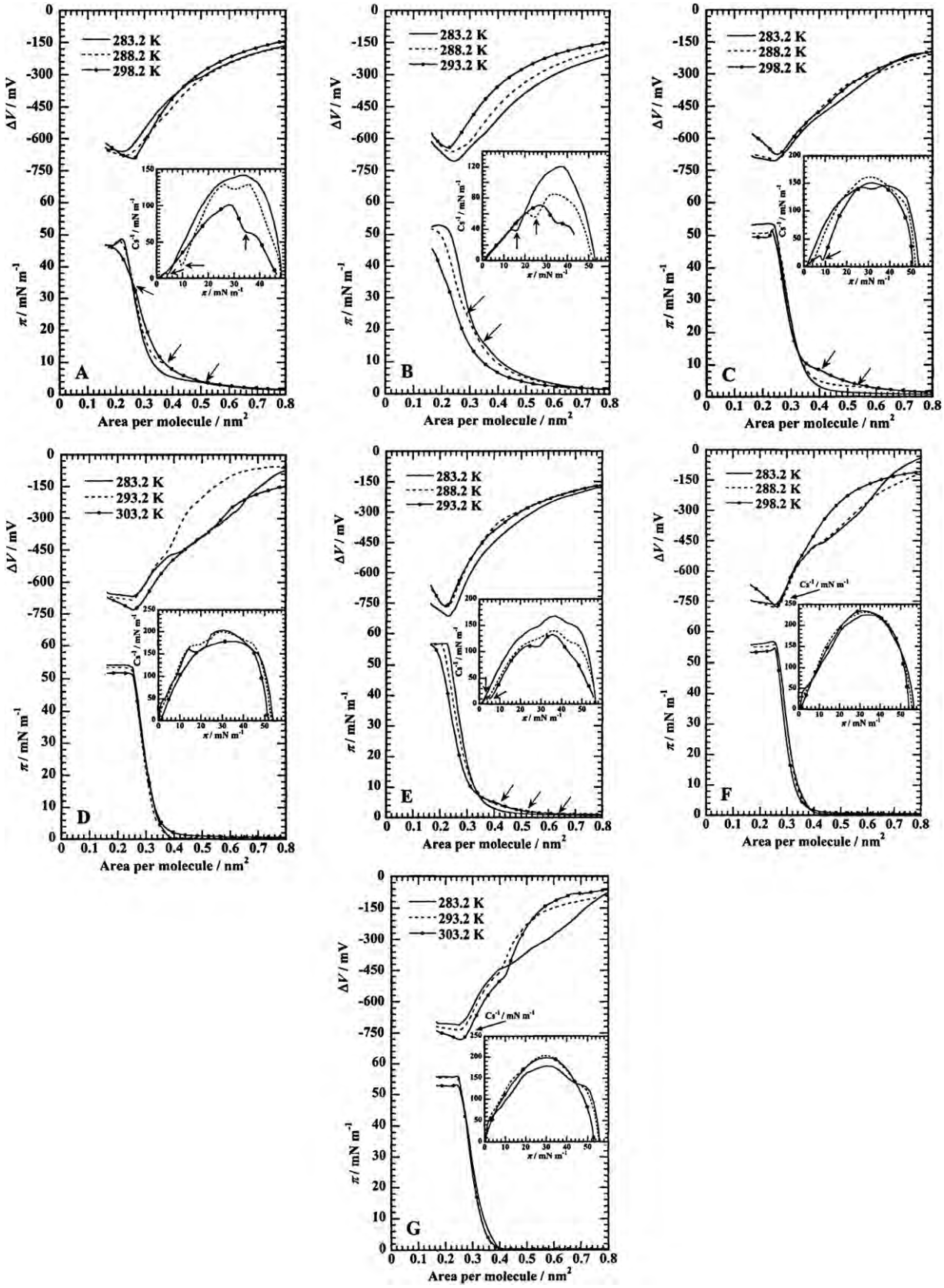

Fig. 4. Surface pressure (π)–molecular area (A) and surface potential (ΔV)–A isotherms of monolayers of (A) *F4H*11OH, (B) *F6H*7OH, (C) *F6H*9OH, (D) *F6H*11OH, (E) *F8H*5OH, (F) *F8H*7OH, (G) *F8H*9OH on water at different temperatures. (Inset) Cs^{-1}–π curves of the corresponding monolayers. The transition pressures (π^{eq}) from disordered to ordered phases are indicated by arrows.

Table 1
Thermodynamic parameters concerning the phase transition from disordered to ordered states on water at different temperatures.

Compounds	Temperature (K)	$\partial\pi^{eq}/\partial T$ (mN m^{-1}K^{-1})	Δs^{γ} (J K^{-1}mol^{-1})	Δh^{γ} (kJ mol^{-1})	T^{c} (K)
*F4H*11OH	283.2	2.0	−240	−68	295.5
	288.2		−79	−23	
	293.2		−26	−8	
	295.2		−3	−1	
	298.2		0	0	
*F6H*7OH	281.2	1.5	−41	−12	290.4
	283.2		−34	−10	
	285.2		−22	−6	
	288.2		−9	−2	
	290.2		−2	−1	
*F6H*9OH	288.2	0.6	−112	−32	302.2
	290.2		−91	−26	
	293.2		−65	−19	
	295.2		−50	−15	
	298.2		−38	−11	
*F8H5*OH	283.2	0.4	−101	−29	297.5
	285.2		−83	−24	
	288.2		−60	−17	
	290.2		−45	−13	
	293.2		−35	−10	

increasing temperatures. In common, the π^{eq} slope against temperature ($\partial\pi^{eq}/\partial T$) for fluorinated amphiphiles is smaller than that for hydrogenated ones due to the thermal resistance of fluorocarbon [28,34,35]. The π^{eq} inclination becomes smaller as the fluorination degree in a molecule increases (Table 1). It has been reported that the slope for the *Hm*OH monolayers (m = 11–14) is ∼1.0 mN m^{-1}K^{-1} regardless of aliphatic chain lengths [36]. Moreover, monolayers of fatty acids such as dodecanoic acid, tridecanoic acid, and tetradecanoic acid also have the similar slope of 1.0–1.2 mN m^{-1}K^{-1} [34]. From these literature data, amphiphiles with a straight-hydrocarbon chain are found to show $\partial\pi^{eq}/\partial T$ of ∼1.0 mN m^{-1}K^{-1}. On the other hand, perfluorocarboxylic acid monolayers have the inclination of 0.2–0.3 mN m^{-1}K^{-1}, which means that perfluorination of hydrocarbon chains in monolayers becomes 3–5 fold thermal resistance [34]. Herein, the slopes of *F6H*9OH and *F8H5*OH monolayers are between those of hydrogenated and perfluorinated analogues as expected. However, *F4H*11OH and *F6H*7OH monolayers are more sensitive to temperature. It is noticed that the thermal sensitivity of *F4H*11OH monolayers is twice as large as that of *Hm*OH monolayers. This demonstrates that the fluorination in molecules is not necessary to induce an addition of the thermal resistance. The obtained slopes can be used to evaluate the apparent molar quantity change on the phase transition as made before [34,37,38], which takes the contribution of the subphase to monolayers into account. The apparent molar entropy change (Δs^{γ}) on the phase transition is derived from the following equation [39]:

$$\Delta s^{\gamma} = (A_C - A_E)\left[\left(\frac{\partial\pi^{eq}}{\partial T}\right)_p - \left(\frac{\partial\gamma^0}{\partial T}\right)_p\right] \quad (2)$$

where A_E and A_C are molecular areas of the expanded (disordered) and the condensed (ordered) phase, respectively. A_E is the area at the onset of the phase transition at the surface pressure π^{eq}. A_C is the extrapolated area of the ordered-state part on the π–A isotherm to π^{eq}. γ^0 is the surface tension of subphase. In the present study, $\partial\gamma^0/\partial T$ of −0.15 mN m^{-1}K^{-1} on water is utilized, which is calculated from the literature data [24]. Moreover, the apparent molar enthalpy change (Δh^{γ}) on the phase transition is calculated by the relation:

$$\Delta h^{\gamma} = T\Delta s^{\gamma} \quad (3)$$

Furthermore, when the Δs^{γ} values are plotted against temperature, the critical temperature T^{c}, above which the monolayer cannot transform into the ordered phase, is obtained by the extrapolation to Δs^{γ} = 0. These resultant thermal parameters are listed in Table 1. All of Δs^{γ} and Δh^{γ} values except for *F4H*11OH at 298.2 K are negative, which respectively means an improvement in the packing of monolayers and an exothermic nature of the phase transition upon compression. Both the values become smaller in magnitude with an increase in temperature. When attention is paid to the total carbon number of 13 (*F6H*7OH and *F8H5*OH), the Δs^{γ} values at the same temperatures suggest that the orientation of *F8H5*OH is more improved than that of *F6H*7OH. In addition, the larger T^{c} value for *F8H5*OH supports the thermal resistance of fluorocarbons. The replacement of two methylene groups with two perfluorinated ones in a molecule is found to increase T^{c} by ∼7 K.

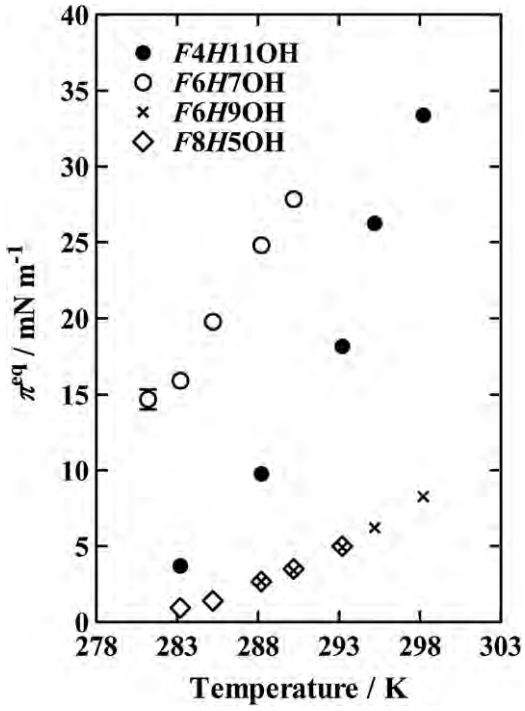

Fig. 5. Plots of the transition pressure (π^{eq}) of *F4H*11OH, *F6H*7OH, *F6H*9OH, and *F8H5*OH monolayers on water as a function of temperature.

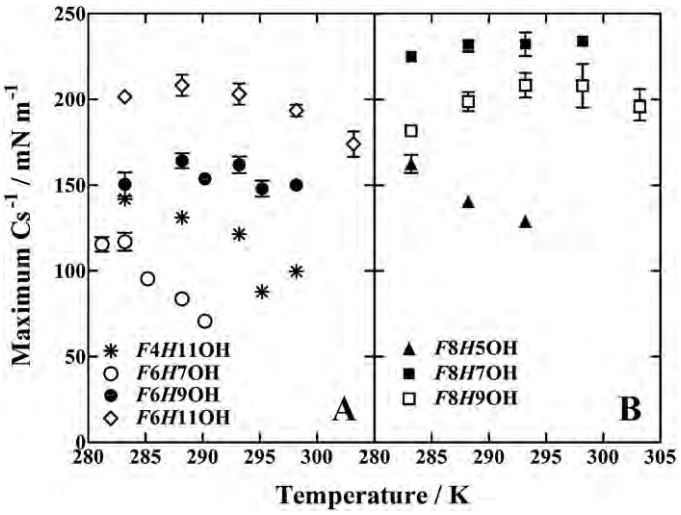

Fig. 6. Plots of the maximum Cs^{-1} value of (A) *F4H*11OH, *F6Hm*OH (m = 7, 9, 11) and (B) *F8Hm*OH (m = 5, 7, 9) monolayers on water as a function of temperature.

Shown in Fig. 6 are the maximum Cs^{-1} values against temperature for the *FnHm*OH monolayers on water. The maximum Cs^{-1} values are obtained from the Cs^{-1}–π curves exhibited in the inset of Fig. 4. As for *F*6*Hm*OH (Fig. 6A), the maximum Cs^{-1} values increase with increasing m. Although *F*6*H*7OH and *F*8*H*5OH are strongly influenced by a change in temperature, the maximum Cs^{-1} values of the others are almost independent of temperature. That is, the following conditions are found to be required to gain the sufficient thermal resistance in a molecule: more than 15 total carbon numbers and perfluorocarbon longer than perfluorohexyl moieties. It is noticed for *F*8*Hm*OH that the values indicate an irregular tendency; *F*8*H*5OH < *F*8*H*9OH < *F*8*H*7OH (Fig. 6B). Generally, there are many differences in physico-chemical property between hydrocarbons and fluorocarbons as mentioned in Section 1. As structural factors, combined effects of cross-section mismatch between *F*-chain and *H*-chain and of repulsive interaction of the dipoles associated to the CF_2–CH_2 linkage are considered to generate such irregular phenomena. Thus, it is demonstrated that determination factors for the elasticity of monolayers are not only the fluorination degree but also the combination and balance of the fluorocarbon and hydrocarbon properties.

4. Conclusion

A series of partially fluorinated alcohols (*FnHm*OH) has been newly synthesized in the present study. In addition, the synthesized compounds, which are highly purified by repeated recrystallizations from acetone/H_2O mixed solvents, are characterized by DSC and the Langmuir monolayer technique. The DSC traces for all the *FnHm*OH exhibit the endothermic peak in the temperature range of 293.2–373.2 K. In particular, a pre-transition (or phase transition of solid) besides the melting peak is observed for *F*6*H*9OH and *F*6*H*11OH. The melting points of *F4H*11OH and *F*6*Hm*OH are lower than those of the corresponding fatty alcohols contrary to our expectations. However, there are few differences in the total enthalpy change (ΔH) between *F*6*Hm*OH and *F*8*Hm*OH. In the isotherm measurement of *FnHm*OH monolayers, it is revealed that disordered/ordered phase transitions of *F4H*11OH and *F*6*H*7OH is more sensitive to temperature than those of the corresponding fatty alcohols. Judging from the fact that perfluorinated molecules and highly fluorinated ones clearly exhibit the thermal stability and resistance, the fluorination in *F4H*11OH and *F*6*Hm*OH exerts the opposite effect to the other *FnHm*OH. The introduction of perfluorobutyl and perfluorohexyl moieties into a molecule might have a strong possibility of a drastic change in its properties such as solubility in solvents, phase behavior, and thermal sensitivity. Unfortunately, however, they have not been thoroughly explained yet. This warrants future work on the incorporation of shorter fluorocarbons involving the relationship to the fluorination degree in a molecule. Nonetheless, the synthesized *FnHm*OH in the present study certainly provides a new insight into functions for the fluorinated molecules, which makes a great impact on materials science, material engineering, and industrial chemistry.

Acknowledgments

This work was supported by a Grant-in-Aid for Scientific Research 23510134 from the Japan Society for the Promotion of Science (JSPS). This work was also supported by a Grant-in-Aid for Young Scientists (B) 22710106 from JSPS and by a Foundation from Oil & Fat Industry Kaikan (H.N.).

Appendix A. Supplementary data

Supplementary data associated with this article can be found, in the online version, at http://dx.doi.org/10.1016/j.colsurfb.2012.08.031.

References

[1] M.P. Krafft, J.G. Riess, Chem. Rev. 109 (2009) 1714–1792.
[2] J.G. Riess, Tetrahedron 58 (2002) 4113–4131.
[3] T.M. Miller, B. Bederson, Adv. Atom. Mol. Phys. 13 (1978) 1–55.
[4] C.P. Higgins, R.G. Luthy, Environ. Sci. Technol. 40 (2006) 7251–7256.
[5] D.C. Burns, D.A. Ellis, H. Li, C.J. McMurdo, E. Webster, Environ. Sci. Technol. 42 (2008) 9283–9288.
[6] K.U. Goss, Environ. Sci. Technol. 42 (2008) 456–458.
[7] J.G. Riess, Curr. Opin. Colloid Interface Sci. 14 (2009) 294–304.
[8] J.G. Riess, Artif. Cells Blood Substit. Immobil. Biotechnol. 33 (2005) 47–63.
[9] J.G. Riess, Artif. Cells Blood Substit. Immobil. Biotechnol. 34 (2006) 567–580.
[10] H. Nakahara, S. Lee, M.P. Krafft, O. Shibata, Langmuir 26 (2010) 18256–18265.
[11] M.P. Krafft, J.G. Riess, Biochimie 80 (1998) 489–514.
[12] M.P. Krafft, Adv. Drug. Deliv. Rev. 47 (2001) 209–228.
[13] J.G. Riess, Chem. Rev. 101 (2001) 2797–2920.
[14] T. Kato, M. Kameyama, M. Ehara, K.-I. Iimura, Langmuir 14 (1998) 1786–1798.
[15] H.-J. Lehmler, M. Jay, P.M. Bummer, Langmuir 16 (2000) 10161–10166.
[16] M. Arora, P.M. Bummer, H.-J. Lehmler, Langmuir 19 (2003) 8843–8851.
[17] O. Shibata, M.P. Krafft, Langmuir 16 (2000) 10281–10286.
[18] H.-J. Lehmler, P.M. Bummer, J. Fluorine Chem. 117 (2002) 17–22.
[19] K. Takai, T. Takagi, T. Baba, T. Kanamori, J. Fluorine Chem. 125 (2004) 1959–1964.
[20] V.M. Sadtler, F. Jeanneaux, M. Pierre Krafft, J. Rabai, J.G. Riess, New J. Chem. 22 (1998) 609–613.
[21] H. Mansour, D.-S. Wang, C.-S. Chen, G. Zografi, Langmuir 17 (2001) 6622–6632.
[22] N.O. Brace, J. Fluorine Chem. 93 (1999) 1–25.
[23] Z. Wang, X. Lu, Tetrahedron 51 (1995) 11765–11774.
[24] W.M. Hayes (Ed.), CRC Handbook of Chemistry and Physics, 91st ed., CRC Press, Boca Raton, London, 2010, p. 2610.
[25] M. Tsuji, T. Inoue, O. Shibata, Colloids Surf. B 61 (2008) 61–65.
[26] G. Nichols, S. Kweskin, M. Frericks, S. Reiter, G. Wang, J. Orf, B. Carvallo, D. Hillesheim, J. Chickos, J. Chem. Eng. Data 51 (2006) 475–482.
[27] H. Nakahara, S. Nakamura, H. Kawasaki, O. Shibata, Colloids Surf. B 41 (2005) 285–298.
[28] Y. Matsumoto, H. Nakahara, Y. Moroi, O. Shibata, Langmuir 23 (2007) 9629–9640.
[29] S. Nakamura, H. Nakahara, M.P. Krafft, O. Shibata, Langmuir 23 (2007) 12634–12644.
[30] P. Dynarowicz-Łatka, M. Pérez-Morales, E. Muñoz, M. Broniatowski, M.T. Martín-Romero, L. Camacho, Phys. Chem. J. B 110 (2006) 6095–6100.
[31] J.T. Davies, E.K. Rideal, Interfacial Phenomena, 2nd ed., New York, Academic Press, 1963.
[32] H. Nakahara, M.P. Krafft, A. Shibata, O. Shibata, Soft Matter 7 (2011) 7325–7333.
[33] R.J. Demchak, T. Fort Jr., J. Colloid Interface Sci. 46 (1974) 191–202.
[34] H. Nakahara, O. Shibata, J. Oleo Sci. 61 (2012) 197–210.
[35] J.G. Riess, M.P. Krafft, Biomaterials 19 (1998) 1529–1539.
[36] D. Vollhardt, G. Emrich, S. Siegel, R. Rudert, Langmuir 18 (2002) 6571–6577.
[37] O. Shibata, Y. Moroi, M. Saito, R. Matuura, J. Colloid Interface Sci. 142 (1991) 535–543.
[38] M. Rusdi, Y. Moroi, S. Nakamura, O. Shibata, Y. Abe, T. Takahashi, J. Colloid Interface Sci. 243 (2001) 370–381.
[39] K. Motomura, T. Yano, M. Ikematsu, H. Matuo, R. Matuura, J. Colloid Interface Sci. 69 (1979) 209–216.